https://doi.org/10.36375/prepare_u.iiche.a377

Degradation of methylene blue through photocatalysis using synthesized ZnO/CeO_2 nanocomposite catalyst

RIPA SUTAR[1], SOMAK JOYTI SAHU[1], LIPIKA DAS SAMANTA[1]*

[1] Department of Chemical Engineering, Haldia Institute of Technology, Haldia, West Bengal-721657, India

**Corresponding author's mail id:lipikadas24@gmail.com*

Abstract:

Nanotechnology is an emerging multidisciplinary technology that has shown tremendous success in a variety of fields. Nanostructures have the potential to improve the physical qualities of traditional textiles in regions such as antibacterial capabilities, water repellence, dirt resistance, colour fastness, and textile material strength. Recent breakthroughs in nanotechnology provide chances to construct next-generation water supply systems by leapfrogging. Nanotechnology-allowed water and wastewater treatment has the probable to not only overcome fundamental challenges confronting current treatment technologies, but also to bring innovative treatment abilities that may allow for the cost-effective exploitation of atypical water sources to increase water supply. The present work focus to degrade the methylene blue (MB) was studied by a photocatalytic process in attendance of ultra violet irradiation using ZnO/CeO_2 nanocomposite catalysts in a batch reactor. The reaction was kept at room temperature. The nano-composite catalyst was synthesized by co-precipitation method using $Zn(NO_3)_2.6H_2O$ and $Ce(NO_3)_3.6H_2O$ as main raw materials. The synthesized catalyst was analyzed by scanning electron microscopy and BET surface area analyzer. After characterization, the catalyst was treated by degrade of methylene blue through photocalysis. The different process conditions such as weight of catalyst, reactant concentration, irradiation time and pH of solution were applied. The effects of energy source and oxidising agent were also investigated. The maximum removal of MB about 99% was achieved using this prepared catalyst.

Keywords: Nano composites; co-precipitation method; photocatalysis; Methylene blue

Introduction:

Colored wastewater from textile mills and food sectors is brilliantly coloured and dangerous. They damage surface and ground water, posing health concerns to animals, plant life, and humans at certain concentrations. Among the chemical pollutants, dyes and dye intermediates, surfactants, and certain metal residues are of particular concern in terms of environmental preservation [1Methylene blue is one such textile effluent (MB). MB dye is harmful to the reproductive and immunological systems [2].

Several conventional processes such as, biological treatment [3, 4], Electrochemical Oxidation [5], activated carbon adsorption [6], Catalytic wet oxidation [7], solvent extraction [8, 9] and membrane process [10, 11] may be employed for the removal of MB. These processes have some major drawbacks such as they are sensitive to operating conditions and tendency to the formation of secondary toxic materials [12]. However, advanced oxidation techniques (AOPs) have recently emerged as a potential method for removing MB from wastewaters. Complete organic matter mineralization is possible in the AOPs [13].

The goal of photocatalysis, a "green" technique, is to completely mineralize organic dyes in wastewater. Heterogeneous photocatalysis using semiconductor oxides and UV-visible light has emerged as a promising method for turning organic pollutants into comparably innocuous end products including CO_2, H_2O, and inorganic ions [14]. In addition, photocatalysis is an excellent option for other conventional ways of water cleanup since it employs a renewable and environmentally friendly source of energy like sunshine [15]. This method degrades toxic organics in the existence of a catalyst and ultraviolet (UV) irradiation without producing additional harmful pollutants. It has been extensively studied during the last few years because of its ablity to totally oxidise organic molecules at a low energy cost [16, 17]. Various novel photocatalytic materials have emerged, such as nano TiO_2 [18, 19], CdS [20], 2D $PbMoO_4$ [21], ZnS [22], ZnO [23] and CaO [24] etc. Zinc Oxide (ZnO) is commonly used as an excellent photocatalyst due to its high activity, low cost, and ability to withstand chemical and photo deterioration. It is non-toxic, has high biological and chemical inertness, and is very stable. When titania is subjected to UV light with an energy larger than its band gap energy, electrons (e) in the conduction band and positive holes (h^+) in the valence band are formed, as well as OH radicals. Pollutant degradation is attributed to OH radicals [25]. Furthermore, ZnO absorbs a bigger fraction of the UV spectrum, is less costly, and has a high potential for organic pollutant removal in water or air [26, 27]. But, one of the significant

https://doi.org/10.36375/prepare_u.iiche.a377

disadvantages as a photocatalyst of ZnO is its high speed of electron-hole recombination, which reduces degradation efficiency. [28]. To address this issue, various teams described doping ZnO with atoms to increase activity [29]. Doping ZnO with a transition metal creates a new energy point in which electrons are trapped, preventing irradiation-induced electron-hole recombination [30, 31]. Metal ion doping in ZnO nanostructures can result in effects such as fluorescence amplification and control of surface defect concentration. Metal doping in ZnO is predicted to change absorbance as well as other physical or chemical characteristics of ZnO [32, 33].

In the present study, ZnO/CeO_2 semiconductor photocatalyst was synthesized by co-precipitation technique. Scanning Electron Microscopy (SEM) and BET Surface Analyzer were applied for characterize the prepared catalyst. The activity of prepared catalyst was observed for the degradation of methylene blue through photocatalytic reaction. The effect of various process parameters such as weight of catalyst, MB concentration variation and pH variation, irradiation time were studied. The kinetic study also studied.

Materials and methods:

Procedure of photocatalyst synthesis

The co-precipitation approach was used to prepare the ZnO/CeO_2 photocatalyst. The major raw ingredients for the catalyst synthesis were $Zn(NO_3)_2.6H_2O$ (Merck Specialties Private Limited, India) and $Ce(NO_3)_3.6H_2O$ (Loba Chemic Private Limited, India). While stirring, the required amounts of $Zn(NO_3)_2.6H_2O$ and $Ce(NO_3)_3.6H_2O$ were mixed for 20 minutes. To adjust pH 10, the necessary quantity of NaOH (Merck Specialties Private Limited, India) was added dropwise and the mixture was agitated for approximately 2 hours. The solution was then let to stand for 24 hours to thoroughly hydrolyze. The resulting sample was extracted and cleaned several periods with distilled water and 100% ethanol to eliminate any excess organic or inorganic contaminants before being dried overnight in a 120°C oven to yield the hydroxide precursors. In a furnace, the dried sample was calcined at 500°C for 6 hours. The composite oxide was finally developed.

Catalyst characterization

Scanning electron microscope (Zeiss, EVO 60) and a BET surface area analyzer (Quantachrome, AUTOSORB 1C, USA) were used to characterise the produced catalyst. The titanium dioxide samples' morphology and particle size were determined using SEM. The specific surface area and pore volume of calcined sample were assessed using a BET surface area analyser.

Experimental Procedure:

The photocatalytic degradation of MB (Merck Specialties Private Limited, India) was investigated using a ZnO/CeO_2 composite catalyst. The reaction took place in a batch cylindrical beaker with a capacity of 1000 ml and continuous stirring, with the UV source placed on top of the reactor. A Philips 8 W UV light with a wavelength of 218 nm was used. A representative reaction was conducted using a 250 ml solution of MB with an initial concentration of 100 ppm and a catalyst concentration of 400 gm/L at 30°C with a 1oC fluctuation using a UV light. The samples were received at regular periods and examined in a UV-VIS spectrophotometer (XPLORER, XP 2001).

Results and Discussions:

Catalyst characterization analysis:

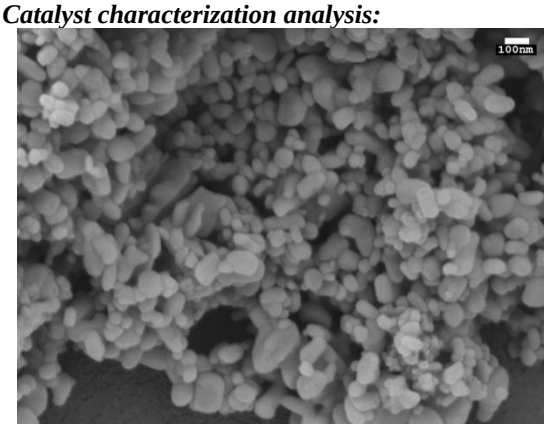

Fig. 1: SEM image of Zno/CeO_2 composite catalyst

The morphology of the composite has been seen in the SEM picture. The catalyst particles are spherical, as seen in Fig. 1. As a result, the SEM picture clearly demonstrates the full homogeneity of cerium with ZnO. Because they may absorb even bulky contaminants, single extremely homogenous aggregates are important for photocatalysis.

The EDS spectrum obtained from SEM was used to identify the quantitative and qualitative composition of the manufactured composite catalyst. Table 1 shows the composition. BET apparatus was used to examine the surface properties of the catalysts. The pore volume and surface area of the produced ZnO catalyst are 147 m^2/g and 0.25 ml/g, respectively. The pore volume and surface area of the produced ZnO/CeO_2 catalyst are 0.81 ml/g and 225 m^2/g, respectively.

Table 1: composition of synthesized ZnO/CeO_2 composite catalyst

Catalyst	Weight (%)		
	Zn	Ce	O
ZnO/CeO_2	46.47	5.39	48.14

Comparison study of various catalysts:

https://doi.org/10.36375/prepare_u.iiche.a377

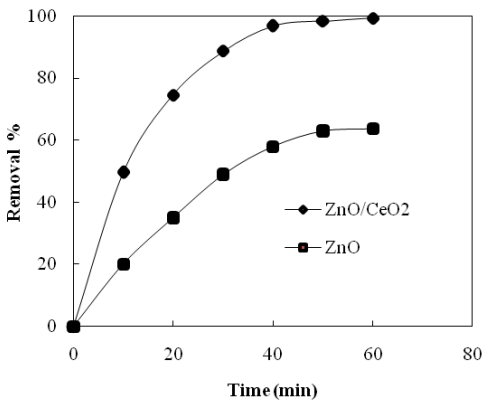

Fig. 2: Effect of various catalysts

Photocatalysis was used to remove MG using different catalysts such as ZnO and ZnO/CeO_2. Both reactions were carried out at 300°C with a 400 mg/L pH 7 catalyst concentrations and a starting concentration of 100 ppm. As shown in Fig. 2, the % removal of MG is in the case of a ZnO/CeO_2 composite catalyst. The removal rate is great due to the large surface area.

The photocatalytic reaction is affected by numerous process factors:

Weight of catalyst:

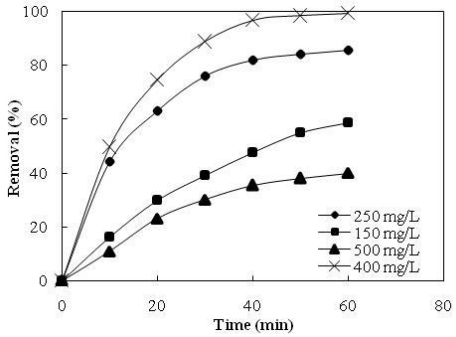

Fig. 3: Effect of catalyst weight on MB degradation

An essential process parameter is the weight of the catalyst driving the photocatalytic reaction. At room temperature, the impact of catalyst concentration on photocatalytic degradation was examined by increasing concentrations from 150 mg/L to 500 mg/L at a starting concentration of MB 100 ppm. Throughout the pH of the MB solution was maintained at 7. Figure 3 depicts the % deterioration over time for various catalyst concentrations. With increasing weight of catalyst up to 400 mg/L, the fraction of MB photocatalytic degradation rises, then decreases. This might be because the number of active sites grows when the quantity of catalyst increases. However, as the catalyst concentration was raised to 400 mg/L, the percentage degradation decreased. It might be due to high-concentration agglomeration of catalyst particles, which reduces the number of active surface sites and hence the removal of MB.

Concentration of dye:

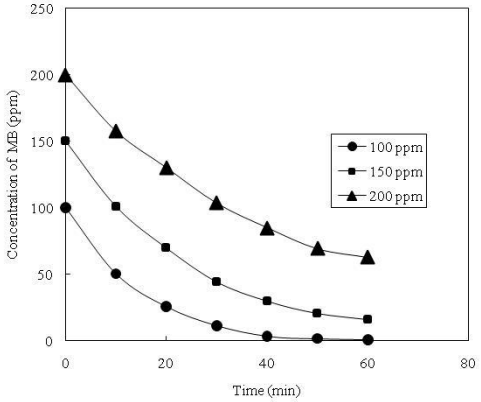

Fig. 4: Effect of dye concentration on MB degradation

Pollutant concentration is a key element in catalytic degradation, and removal effectiveness is dependent on the starting concentration of the substrate. The reactions were studied at 30 ^oC with a catalyst concentration of 400 mg/L and a pH of 7. Figure 4 depicts the concentration of MB as a function of time with regard to varied beginning concentrations of the MB dye solution (100 mg/L to 200 mg/L). These data demonstrate that the dye degrades rapidly even at modest beginning concentrations (100 mg/L). The % elimination of MB reduces as the starting concentration of the dye increases. It has been discovered that utilising modest dye concentrations, virtually full elimination is feasible. At 60 minutes, the percentage degradation of MB at a concentration of 100 mg/L is found to be 99%, whereas at a concentration of 200 mg/L it is 62%. The likely explanation for the reduction in percent degradation with increasing initial dye concentration is that when the opening concentration of MB increases, the number of dye molecules increases, making light penetration more difficult. The dye molecules do not dissolve instantaneously because the intensity of the light and the amount of catalyst do not increase. The solution colour becomes more vivid as the dye concentration increases, and photons entering the solution have a shorter path length, enabling fewer photons to reach the photocatalyst surface. Furthermore, the generation of hydroxyl radical decrease. According to the Beer-Lambert equation, the path length of photons coming into the solution shortens as the initial dye concentration increases, resulting in less photon adsorption on catalyst surfaces and, as a result, a lower photo degradation rate..

https://doi.org/10.36375/prepare_u.iiche.a377

pH:

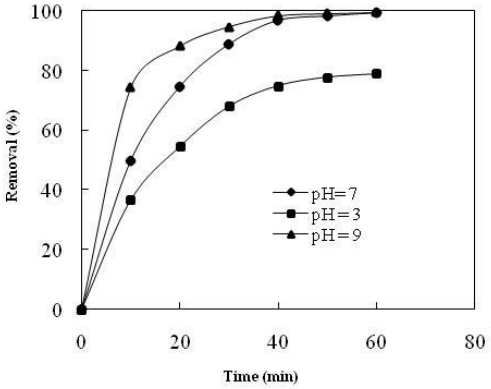

Fig. 5: Effect of pH on MB degradation

The pH of the original MB solution is 7. To modify the pH of the solution, dilute hydrochloride acid or sodium chloride solutions were utilised. The reactions were studied by varying the pH from 3 to 9 and starting with a concentration of MB 100 mg/L for a catalyst concentration of 400 mg/L. According to Fig. 5, the % removal of MB increases as the pH of the solution medium increases. When dissolved in water, MB, on the other hand, becomes a cationic dye. Adsorption was not typical at low pH (pH = 3). However, when the pH of the solution climbed from 3 to 9, more MB was adsorbed on the catalyst face, with the pH range of 9 showing the greatest dye absorption. The positively charged surfaces of the catalyst resisted cationic adsorbate species adsorption in acidic environments due to the surface of the dye solution tends to acquire a negative charge when the pH of the dye solution increases due to the growing electrostatic desirability between the positively charged dye and the negatively charged catalyst.

Time of irradiation:

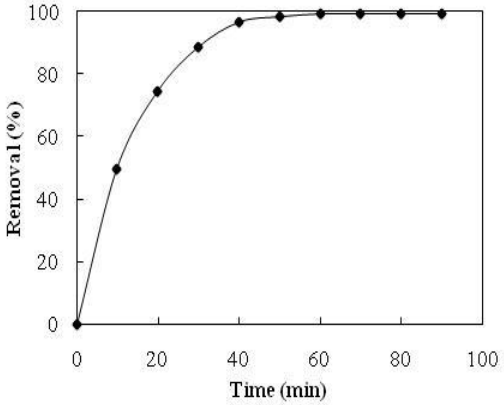

Fig. 6: Effect of reaction time on MB degradation

The impact of irradiation period on photocatalytic degradation of MB in its aqueous solution was studied from 0 to 90 minutes with weight of catalyst 400 mg/L at 100 mg/L MB concentration. The pH was maintained of 7during reaction at room temperature and the outcome is depicted in Fig. 6. The data clearly demonstrate that photodegradation efficiency rises with time up to 50 minutes and then plateaus. This suggests that photocatalytic MB degradation with catalysts for 60 minutes is the best irradiation time.

The effect of the energy source and the oxidizing agent:

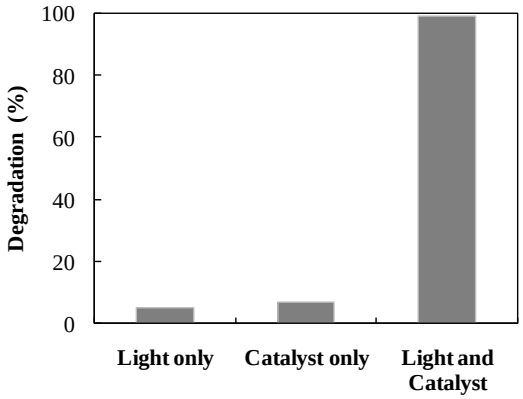

Fig. 7: Effect of energy source and oxidizing agent on MB degradation

The presence of an oxidising agent ZnO/CeO_2 catalyst and UV light as an energy source was shown to improve dye solution degradation. The reactions were carried out using a starting concentration of MB 100 mg/L and a catalyst concentration of 400 mg/L. Figure 7 depicts the nature of photo deterioration. By adding catalyst, dye was eliminated 99% after 60 minutes of UV irradiation at room temperature, but only 5% after UV irradiation without catalyst. When the catalyst was utilised in the dark, there were no changes in dye concentration (6.96%) without UV irradiation. Thus, both UV light and the photocatalyst catalytic are required for effective MB breakdown. When a catalyst absorbs UV light, it generates pairs of electrons and holes. The electron in titanium dioxide's valence band is excited. The excited electron's surplus energy propelled it to the catalyst's conduction band, where it produced a pair of negative electrons (e-) and positive holes (h+). The positive hole in the catalyst separates the water molecule, resulting in the formation of the hydroxyl radical. This hydroxyl radical is dependable for colour degradation.

Kinetic study:

In heterogeneous reactions, the catalyst surface plays an important role. Previous literatures [34, 35] show that the modified Langmuir-Hinshelwood (L-H) kinetic appearance is effectively used to study the heterogeneous photocatalysis.

During the solid catalytic process, water molecules continually cover the surface of the ZnO/CeO2 composite, and water and MB molecules compete for a single adsorption site. The active sites will be coated with MB and water molecules, and the fraction of surface coverage will be determined. The initial concentration of MB and water molecules is given by [36]:

https://doi.org/10.36375/prepare_u.iiche.a377

$$\emptyset = \frac{K_{MB}C_0}{(1+K_{MB}C_0+k_WC_W)} \quad \text{Eq. (1)}$$

where $\emptyset$ is the fraction of surface covered by MB molecules. K_{MB} and k_W are the adsorption equilibrium constant of MB and water, respectively. C_0 and C_W are the initial concentrations of MB and water, respectively. $\emptyset$ may be written as,

$$\emptyset = \frac{\left[\frac{K_{MB}}{1+k_WC_W}\right]C_0}{1+\left[\frac{K_{MB}}{1+k_WC_W}\right]C_0} \quad \text{Eq. (2)}$$

During the reaction time, the initial concentration of water (C_W) can be considered to be constant. As a result, by introducing a new constant, $\emptyset$ is simplified. $K_1 = \left[\frac{K_{MB}}{1+k_WC_W}\right]$

Equation 2 can be rewritten as

$$\emptyset = \frac{K_1C_0}{1+K_1C_0} \quad \text{Eq. (3)}$$

According to Langmuir-Hinshelwood (L-H), the rate of reaction (-rA) is proportional to the fraction of the substrate's surface covered ($\emptyset$):

$$-r_A = k_C\emptyset \quad \text{Eq. (4)}$$

With Eq. (3) and Eq. (4), we get

$$-r_A = \frac{K_1k_c[C_0]}{1+K_1[C_0]} \quad \text{Eq. (5)}$$

Eq. (5) is linearized in the following form

$$\frac{C_0}{-r_A} = \frac{1}{K_1k_c} + \frac{C_0}{k_C} \quad \text{Eq. (6)}$$

The slope of the concentration profile's tangent at t = 0 was used to calculate the starting rate data. After translating to their respective variable, the initial rate data were fitted in Eq. (6). Figure 8a shows a typical plot of $C_0/-r_A$ vs C_0 at various catalyst loadings.

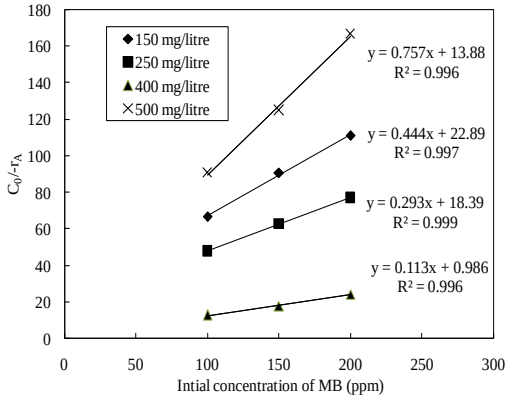

a

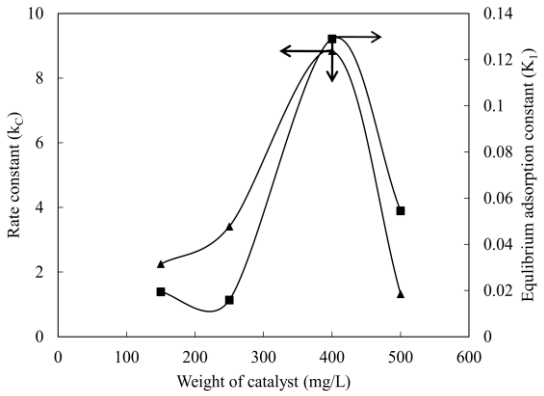

b

Fig. 8 (a) Relation between $C_0/-r_A$ and C_0 at various catalysts weight and **(b)** the rate constant (k_c) and the adsorption equilibrium constant (K_1) as a role of catalyst weight

The rate data fit to the linear equation adequately for MB concentrations of 100-300 ppm, with high correlation coefficients. Figure 8b depicts the dependence of k_c and the constant K_1 on catalyst loading. The rate constant k_c rises proportionately with increasing catalyst loading in the range 250-400 mg/L, then drops. However, K_1 steadily increases as catalyst loading increases.

As shown in Fig. 3, the percentage removal is affected by catalyst loading. The rate constant (k_c) appears to progressively increase with catalyst amount up to 400 mg/L, then decrease with further addition of catalyst quantity due to reduction in K_1. Constant K_1 drops with increasing catalyst weight, possibly due to a decrease in surface area. The reduction in surface area might be due to the agglomeration of a huge number of catalyst particles. The lesser the quantity of adsorbed substrate, then slower the breakdown rate. It is possible to infer that both the pseudo first-order and Langmuir-Hinshelwood type models may describe the rate kinetics of MB photo removal employing a ZnO/CeO_2 catalyst.

Conclusions:

The ZnO nano compound, which is widely utilized as a photocatalyst for the degradation of organic coloured dyes, has been modified with CeO2 doping for visible light activation. The ZnO/CeO_2 catalyst was successfully synthesized by co-precipitation method. The catalyst was large surface area and spherical in shape with good homogeneity. The prepared catalyst was used for degradation of MB during photocatalytic process. The reaction was carried out various process parameters. Almost 99% removal of MB achieved at 400 mg/L catalyst loading with an initial concentration of MB 100 mg/L at pH 7 under room temperature. The removal of MB was studied in absence of catalyst and energy source (UV-C). So Therefore, the composite

catalyst is a good candidate in the handling of industrial wastewater to eliminate dye, which causes severe risk to environment.

References:

[1] Parshetti, G; Kalme, S; Saratale, G;. Govindwar, S. Biodegradation of malachite green by Kocuria rosea MTCC 1532. Acta. Chim. Slov. 2006, 53, 492–498.
DOI: 10.4236/ojbm.2022.103058
[2] Oturan, M.A; Guivarch, E; Oturan, N; Sires, I. Oxidation pathways of malachite green by Fe^{3+}-catalyzed electro-Fenton process. Appl. Catal. B. 2008, 82, 244–254.
DOI:10.1016/j.apcatb.2008.01.016
[3] Mulugeta, M; Lelisa, B. Removal of Methylene Blue (Mb) Dye from Aqueous Solution by Bioadsorption onto Untreated Parthenium hystrophorous Weed. Modern. Chemistry. & Applications. 2014, 2(4), 1-5.
DOI: 10.4172/2329-6798.1000146
[4] Cheng, M; Zeng, G; Huang, D; Lai, C; Wei, Z; Li, N; Xu, P; Zhang, C; Zhu, Y; He, X. Combined biological removal of methylene blue from aqueous solutions using rice straw and Phanerochaete chrysosporium. Appl. Microbiol. Biotechnol. 2015, 99(12), 5247-56.
DOI: 10.1007/s00253-014-6344-9
[5] Asghar, H.M.A; Ahmad, T; Hussain, S.N; Sattar, H. Electrochemical Oxidation of Methylene Blue in Aqueous Solution. Int. J. Chem. Eng. Appl. 2015, 6(5), 352-355.
DOI: 10.7763/IJCEA.2015.V6.508
[6] Kareem, A; Alrazak, N.A; Aljebori, K.H; Aljeboree, A.M; Algboory, H.L; Alkaim, A.F. Removal of methylene blue dye from aqueous solutions by using activated carbon/ureaformaldehyde composite resin as an adsorbent. Int. J. Chem. Sci. 2016, 14(2), 635-648.
DOI: 10.2166/wst.2015.450
[7] Das, M; Bhattacharya, K.G. Use of Raw and Acid-Treated MnO_2 as Catalysts for Oxidation of Dyes in Water: A Case Study with Aqueous Methylene Blue. Chem. Eng. Commun. 2015, 202(12), 1657-1667.
DOI:
https://doi.org/10.1080/00986445.2014.968715
[8] El-Ashtoukhy, E.S.Z; Fouad, Y.O. Liquid–liquid extraction of methylene blue dye from aqueous solutions using sodium dodecylbenzenesulfonate as an extractant. Alex. Eng. J. 2015, 54, 77–81.
DOI: https://doi.org/10.1016/j.aej.2014.11.007
[9] Muthuraman, G; Teng, T.T; Leh, C.P; Norli, I. Extraction and recovery of methylene blue from industrial wastewater using benzoic acid as an extractant. J. Hazard. Mater. 2009,163, 363–369.
DOI: 10.1016/j.jhazmat.2008.06.122
[10] Ashraf, M.W. Removal of methylene blue dye from wastewater by using supported liquid memberane technology. Pol. J. Chem. Technol. 2016, 18(2), 1-5.
DOI: 10.1515/pjct-2016-0025
[11] Banata, F; Al-Asheh, S; Qtaishat, M. Treatment of waters colored with methylene blue dye by vacuum membrane distillation. Desalination 2005, 174(1), 87-96.
DOI: 10.1016/J.DESAL.2004.09.004
[12] Busca, G; Berardinelli, S; Resini, C; Arrighi, L. Technologies for the removal of phenol from fluid streams: A short review of recent developments. J. Hazard. Mater. 2008, 160(2-3), 265–288.
DOI: 10.1016/j.jhazmat.2008.03.045
[13] Nogueira, A.E; Castro, I.A; Giroto, A. S; Magrioti,s Z.M. Heterogeneous Fenton-Like Catalytic Removal of Methylene Blue Dye in Water Using Magnetic Nanocomposite (MCM-41/Magnetite). J. Catal. 2014, 4, 1-6.
DOI: https://doi.org/10.1155/2014/712067
[14] Rizzo, L; Koch, J; Belgiorno, V; Anderson, M.A. Removal of methylene blue in a photocatalytic reactor using polymethylmethacrylate supported TiO_2 nanofilm. Desalination. 2005, 211(1-3), 1-9.
DOI: 10.1016/j.desal.2006.02.081
[15] Zhang, X; Wang, Y; Liu, B; Sang, Y; Liu, H. Heterostructures construction on TiO_2 nanobelts: A powerful tool for building high-performance photocatalysts. Appl. Catal. B. 2017, 202, 620–641.
DOI: https://doi.org/10.1016/j.nanoso.2022.100858
[16] Linsebigler, A.L; Lu, G; Jr., J.T.Y. Photocatalysis on Titania surfaces: principles, mechanisms, and selected results. Chem. Rev. 1995, 95(3), 735-758.
DOI: https://doi.org/10.1016/j.apcatb.2016.09.068
[17] Robertson, P.K.J. Semiconductor photocatalysis: an environmentally acceptable alternative production technique and effluent treatment process. J. Clean. Prod. 1996, 4(3-4), 203-212.
DOI:https://doi.org/10.1016/S09596526(96)00044-3
[18] Prado, A.G; Costa, L.L. Photocatalytic decouloration of malachite green dye by application of TiO_2 nanotubes. J. Hazard. Mater. 2009, 169(1-3), 297-301.
DOI: 10.1016/j.jhazmat.2009.03.076
[19] Yongmei, Ma; Maofei, Ni; Siyue, Li. Optimization of Malachite Green Removal from Water by TiO_2 nanoparticles under UV Irradiation. Nanomaterials 2018, 8(6), 428.
DOI: 10.3390/nano8060428
[20] Sethi, Y.A; Panmand, R.P; Kadam, S.R; Kulkarni, A.K; Apte, S.K; Naik, S.D; Munirathnam, N; Kulkarni, M.V; Kale, B.B. Nanostructured CdS sensitized $CdWO_4$ nanorods for hydrogen generation from hydrogen sulfide and

dye degradation under sunlight. J. Colloid. Interface. Sci. 2017, 487, 504–512.
DOI: 10.1016/j.jcis.2016.10.063
[21] Robi, S.D; Jian, Z; Md, M; Benjamin, J.C; Torben, D. Two dimensional $PbMoO_4$: A photocatalytic material derived from a naturally non-layered crystal. Nano. Energy. 2017, 49, 237–246.
DOI: https://doi.org/10.3390/ma11061004
[22] Muslim, Z.R; Kadhim, R.F. Photocatalytic removal of methylene blue dye by using of ZnS and CdS. Iraqij. Appl. Phys. 2017, 15(33), 11-16.
DOI: https://doi.org/10.30723/ijp.v15i33.135
[23] Muslim, Z.R; Aadim, K.A; Kadhim, R.F. Preparation of ZnO for Photocatalytic Activity of Methylene Blue Dye. Int. J. Basic. Appl. Sci. 2017, 6(1), 1-7.
DOI: https://doi.org/10.1155/2021/5201497
[24] Ameta, R; Kumar, D; Jhalora, P. Photocatalytic degradation of methylene blue using calcium oxide. Acta. Chimica. and Pharmaceutica. Indica. 2014, 4(1), 20-28.
DOI: 10.1002/slct.202003046
[25] Karunakaran, C; Dhanalakshmi, R; Gomathisankar, P;, Manikandan, G. Enhanced phenol-photodegradation by particulate semiconductor mixtures: Interparticle electron-jump. J. Hazard. Mater. 2010, 174 (1-3), 799-806.
DOI: 10.1016/j.jhazmat.2009.11.105
[26] Dong, S; Xu, K; Liu, J; Cui, H. Photocatalytic performance of ZnO:Fe array films under sunlight irradiation. Phys. B. Condens. Matter. 2011, 406, 3609-3612.
DOI:10.1016/j.physb.2011.06.053
[27] Kumar, K; Chitkara, M; Sandhu, I.S; Mehta, D; Kumar, S. Photocatalytic, optical and magnetic properties of Fe-doped ZnO nanoparticles prepared by chemical route. J. Alloys. Compd. 2014, 588, 681-689.
DOI: 10.1016/j.jallcom.2013.11.127
[28] Nirmala, M; Nair, M.G; Rekha, K; Aunkaliani, A; Samdarshi, S.K; Nair, R.G. Photocatalytic activity of ZnO nanopowders synthesized by DC thermal plasma. African. Journal. of Basic. & Applied. Sciences. 2010, 2, 161-166.
DOI:http://dx.doi.org/10.1016/j.matlet.2011.03.079
[29] Yanfa, Y; Al-Jassim, M.M, Wei, S. Doping of ZnO by group-IB elements. Appl. Phys. Lett. 2006, 89(18), 181912-181912.
DOI:10.1063/1.2378404

[30] Xing, G.Z; Tao, J.G; Li, G.P; Zhang, Z; Wong, L.M; Wang, S.J; Huan, C.H.A; Wu, T. Doping Cu into ZnO Nanostructures. 2nd IEEE International. Nanoelectronics. Conference. Shanghai, China, 2008.
DOI:10.1109/INEC.2008.4585528
[31] Zhang, Y; Ram, M.K; Stefanakos, E.K; Guwami, D.Y. Enhanced photocatalytic activity of iron doped zinc oxide nanowires for water decontamination. Surf. Coat. 2013, 217, 119-123.
DOI: 10.1016/J.SURFCOAT.2012.12.001
[32] Umar, K; Aris, A; Parveen, T; Jaafar, J; Majid, A.Z; Reddy, A.V.B; Talib, J. Synthesis, characterization of Mo and Mn doped ZnO and their photocatalytic activity for the decolorization of two different chromophoric dyes. Appl. Catal. A-Gen. 201, 505, 507-514.
DOI: 10.1016/j.apcata.2015.02.001
[33] Ahmed, S.A. Structural, optical, and magnetic properties of Mn-doped ZnO samples. Results. Phys. 2017, 7, 604-610.
DOI: https://doi.org/10.1016/j.rinp.2017.01.018
[34] Morales, G.V; Sham, E.L; Cornejo, R; Farfan, Torres, M.E. Photocatalytic degradation of 2-chlorophenol by TiO_2: kinetic studies. Lat. Am. Appl. Res. 2013, 43, 325-328.
DOI: S0327-07932013004400006
[35] Tang, W.Z; An, H. Photocatalytic degradation kinetics and mechanism of acid blue 40 by TiO_2/UV in aqueous solution. Chemosphere 1995, 31(9), 4171-4183.
DOI: https://doi.org/10.1016/0045-6535(95)80016-E
[36] Sun, P; Zhang, J; Liu, W; Wang, Q; Cao W. Modification to L-H Kinetics Model and Its Application in the Investigation on Photo degradation of Gaseous Benzene by Nitrogen-Doped TiO_2. Catalysts. 2018, 8, 1-14.
DOI:https://doi.org/10.3390/catal8080326